All-Organometallic Analogues of Zeise's Salt for the Three Group 10 Metals

Juan Forniés,* Antonio Martín, L. Francisco Martín, and Babil Menjón

Instituto de Ciencia de Materiales de Aragón, Facultad de Ciencias, Universidad de Zaragoza-CSIC, C/ Pedro Cerbuna 12, E-50009 Zaragoza, Spain

Athanassios Tsipis*

Laboratory of Inorganic and General Chemistry, Department of Chemistry, University of Ioannina, Ioannina 451 10, Greece

Received March 18, 2005

Ethene has been found to be able to split the electron-deficient pentafluorophenyl bridging system in $[NBu_4]_2[\{M(C_6F_5)_2\}(\mu\text{-}C_6F_5)_2]$ to give the corresponding mononuclear compounds $[NBu_4][M(C_6F_5)_3(\eta^2\text{-}C_2H_4)]$ (M = Pt (**1**), Pd (**2**)) in reasonable yield. Compounds **1** and **2** are well-behaved species and have been isolated and characterized by analytical and spectroscopic methods. The crystal structure of **2**, as established by X-ray diffraction methods, reveals that the Pd atom is in an approximately *SP*-4 environment defined by the *ipso*-C atoms of the three σ-bound C_6F_5 groups ($C_6F_5\text{-}\kappa^1$) and the midpoint between the doubly bonded C atoms of the metal π-bound ethene molecule ($\eta^2\text{-}C_2H_4$). The ethene molecule is coordinated upright, and the C=C bond length (133.6(6) pm) is the same as in the free ligand (133.7(2) pm). The nickel homologue $[NBu_4][Ni(C_6F_5)_3(\eta^2\text{-}C_2H_4)]$ (**3**), formed by the low-temperature reaction of $[NBu_4]_2[Ni(C_6F_5)_4]$ with $B(C_6F_5)_3$ in the presence of C_2H_4, could not be isolated but only spectroscopically detected in solution. The experimentally established stability of the $[M(C_6F_5)_3(\eta^2\text{-}C_2H_4)]^-$ species has been found to follow the trend calculated by DFT methods for the M-(η^2-C_2H_4) bond strength: Pt > Pd > Ni. Furthermore, quantitative estimates of back-bonding in the $[M(C_6F_5)_3(\eta^2\text{-}C_2H_4)]^-$ and $[MCl_3(\eta^2\text{-}C_2H_4)]^-$ anions were obtained using NBO analyses of electron populations of the relevant donor−acceptor orbitals and the second-order stabilization energy associated with the charge transfer (CT) interactions describing the back-bonding phenomenon.

Introduction

In the first half of the 19th century, Zeise prepared and isolated potassium and ammonium salts of the $[PtCl_3(\eta^2\text{-}C_2H_4)]^-$ anion,[1] which have been generally acknowledged to be the first organometallic species ever isolated in analytically pure form and reported in the scientific literature.[2] Although the initial formulation of the potassium salt—usually referred to as *Zeise's salt*—as an ethene derivative was challenged by Liebig,[3] the discoverer stood by his original opinion,[4] a point of view that was later confirmed by independent work.[5] The constitutional nature of the complex anion $[PtCl_3(\eta^2\text{-}C_2H_4)]^-$ as well as that of its bromo analogue[6] was, however, not fully understood until much later, thanks to the model formulated by Dewar to rationalize the olefin-to-metal bond[7] that was shortly thereafter applied to the platinum case by Chatt and Duncanson.[8] The molecular structure of Zeise's anion was definitely established by three-dimensional single-crystal X-ray[9] and neutron diffraction methods.[10]

The analogous palladium derivative $[PdCl_3(\eta^2\text{-}C_2H_4)]^-$ is considered to be a key intermediate species in the Pd-catalyzed oxidation of ethene (Wacker process)[11] and has been spectroscopically detected in solution of nonprotic solvents.[12] The corresponding $[NBu_4]^+$ salt was claimed to have been isolated as a pale yellow solid that lost

* To whom correspondence should be addressed. E-mail for J.F.: juan.fornies@unizar.es. E-mail for A.T. (for comments concerning the theoretical calculations): attsipis@cc.uoi.gr.

(1) Zeise, W. C. *Ann. Phys. Chem.* **1831**, *21*, 497, 542.

(2) Seyferth, D. *Organometallics* **2001**, *20*, 2. Thayer, J. S. *Adv. Organomet. Chem.* **1975**, *13*, 1. Thayer, J. S. *J. Chem. Educ.* **1969**, *46*, 442.

(3) Liebig, J. *Ann. Pharm.* **1834**, *9*, 1. Liebig, J. *Ann. Phys. Chem.* **1834**, *31*, 321. Liebig, J. *Ann. Pharm.* **1837**, *23*, 12.

(4) Zeise, W. C. *Danske Selsk. Skr.* **1837**, *6*, 333. Zeise, W. C. *Ann. Phys. Chem.* **1837**, *40*, 234. Zeise, W. C. *Ann. Pharm.* **1837**, *23*, 1.

(5) Griess, P.; Martius, C. A. *Ann. Chem.* **1861**, *120*, 324. Birnbaum, K. *Ann. Chem.* **1868**, *145*, 68. Anderson, J. S. *J. Chem. Soc.* **1934**, 971. Gel'man, A. D.; Litvak, I. B. *Izv. Plat.* **1939**, *16*, 29.

(6) Chojnacki, C. *Z. Chem.* **1870**, 419.

(7) Dewar, M. J. S. *Bull. Soc. Chim. Fr.* **1951**, C71. For Dewar's comment on this subject, see: Dewar, M. J. S.; Ford, G. P. *J. Am. Chem. Soc.* **1979**, *101*, 783. For a historical perspective on the effect of Dewar's bonding model for metal−alkene complexes on the development of organometallic chemistry, see: Mingos, D. M. P. *J. Organomet. Chem.* **2001**, *635*, 1.

(8) Chatt, J.; Duncanson, L. A. *J. Chem. Soc.* **1953**, 2939. See also: Leigh, G. J. *Coord. Chem. Rev.* **1991**, *108*, 1.

(9) Jarvis, J. A. J.; Kilbourn, B. T.; Owston, P. G. *Acta Crystallogr., Sect. B* **1971**, *27*, 366. Black, M.; Mais, R. H. B.; Owston, P. G. *Acta Crystallogr., Sect. B* **1969**, *25*, 1753. In these papers, reference to previous studies by two-dimensional X-ray diffraction methods can also be found.

(10) Love, R. A.; Koetzle, T. F.; Williams, G. J. B.; Andrews, L. C.; Bau, R. *Inorg. Chem.* **1975**, *14*, 2653.

(11) Jira, R. In *Applied Homogeneous Catalysis with Organometallic Compounds*; Cornils, B., Herrmann, W. A., Eds.; Wiley-VCH: Weinheim, Germany, 2000; Section 2.4.1, pp 374−393.

10.1021/om0502077 CCC: $30.25
Publication on Web 06/08/2005

C_2H_4 fairly rapidly at room temperature, but no analytical or any other solid-state data were provided.[12d] The nickel derivative, $[NiCl_3(\eta^2\text{-}C_2H_4)]^-$, has, to the best of our knowledge, never been detected. The decrement in information about the $[MCl_3(\eta^2\text{-}C_2H_4)]^-$ species for the group 10 metals on going from Pt to Ni might be related to the M−alkene bond energy, which, according to recent theoretical calculations, has been estimated to sharply decrease in the order Pt (33.9 kcal mol^{-1}) > Pd (19.0 kcal mol^{-1}) > Ni (6.1 kcal mol^{-1}).[13]

The C_6F_5 group has been assigned an electron-withdrawing character only slightly weaker than that exerted by the chloro ligand.[14] In our experience, however, the C_6F_5 group has a number of other properties that, in some instances, make this ligand advantageous over Cl^-. Thus, the higher steric requirements of C_6F_5 may exert a shielding effect toward other coordinated ligands as well as toward vacant coordination sites.[15] Moreover, metal-coordinated Cl and C_6F_5 ligands exhibit very different dissociation abilities, but perhaps the most distinctive difference may be the much lower residual nucleophilic character of metal-coordinated C_6F_5 groups compared to that of metal-coordinated chloro ligands. Considering that all these properties could add to favor the stabilization of metal-coordinated ethene and encouraged by our success in isolating and characterizing the complete series of square-planar carbonyl derivatives *cis*-$[M(C_6F_5)_2(CO)_2]$ (M = Ni, Pd, Pt),[16] we sought to prepare salts of the $[M(C_6F_5)_3(\eta^2\text{-}C_2H_4)]^-$ anions for all three group 10 metals. The results obtained are reported and discussed in the present paper. Moreover, the key factors determining the stability of the novel Zeise type salts have been inferred by electronic structure calculation methods at the DFT level of theory, while quantitative estimates of back-bonding were obtained using NBO analyses of electron populations of the relevant donor−acceptor orbitals and the second-order stabilization energy associated with the charge transfer (CT) interactions describing the back-bonding phenomenon.

Results and Discussion

The reaction of the anionic homoleptic species $[NBu_4]_2[M(C_6F_5)_4]$ (M = Pt, Pd) with the corresponding solvento derivatives *cis*-$[M(C_6F_5)_2(THF)_2]$ is known to proceed with extrusion of the very labile THF ligands and formation of the homodinuclear compounds $[NBu_4]_2[M_2(C_6F_5)_6]$ (Scheme 1).[17] In these latter homoleptic species, four C_6F_5 groups act as terminal σ-bound ligands, while the remaining two build an electron-deficient, doubly bridging system: $[NBu_4]_2[\{M(C_6F_5)_2\}_2(\mu\text{-}C_6F_5)_2]$.[17,18] Although several alkyl and aryl groups (e.g. Me, Et, Ph, mesityl, ...) are known to be able to form [3c,2e] bonds with main-group elements as well as with transition metals, the case of the C_6F_5 group is especially remarkable because of its high electron-withdrawing character.[14] Indeed, the pentafluorophenyl derivatives $[NBu_4]_2[\{M(C_6F_5)_2\}_2(\mu\text{-}C_6F_5)_2]$ show interesting reactivity patterns associated with the electron-deficient bridging system, including different redox processes and addition of electrophiles to the *para* position of the C_6F_5 ring.[19] In addition, a good number of donor ligands are known to cause the splitting of the bridging system that can occur in a symmetric or an asymmetric way (Scheme 1), depending on the nature of the metal and of the ligand used.[17,20] We will now discuss the results obtained when L = C_2H_4.

Scheme 1

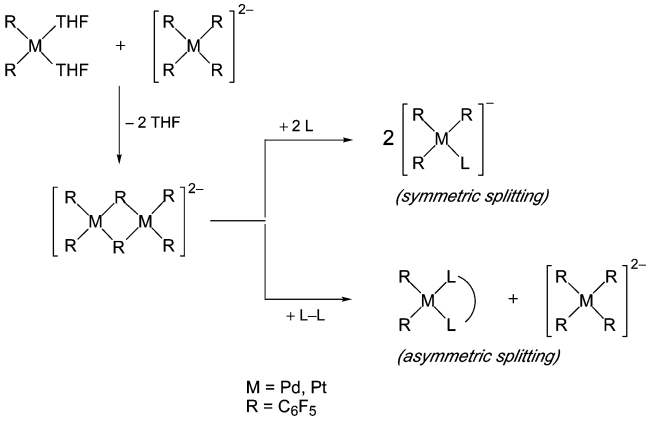

Scheme 2

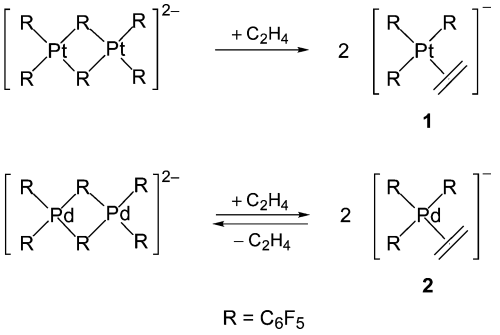

Synthesis and Characterization of $[NBu_4][Pt(C_6F_5)_3(\eta^2\text{-}C_2H_4)]$ (1). Bright yellow CH_2Cl_2 solutions of $[NBu_4]_2[\{Pt(C_6F_5)_2\}_2(\mu\text{-}C_6F_5)_2]$ gradually turn colorless when put under an ethene atmosphere at room temperature. This change in color is due to the symmetric splitting of the bridging system (Scheme 2), as clearly seen by ^{19}F NMR spectroscopy: the low-field resonances characteristic of bridging C_6F_5 groups disappear upon exposure to C_2H_4, giving rise to two sets of signals in a 2:1 ratio which are typical of square-planar (*SP*-4) $[Pt(C_6F_5)_3(L)]^-$ species. The signal corresponding to the *ortho* F atoms of the *trans*-to-ethene C_6F_5 group

(12) (a) Bencze, É.; Pápai, I.; Mink, J.; Goggin, P. L. *J. Organomet. Chem.* **1999**, *584*, 118. (b) Olsson, A.; Kofod, P. *Inorg. Chem.* **1992**, *31*, 183. (c) Olsson, L.-F.; Olsson, A. *Acta Chem. Scand.* **1989**, *43*, 938. (d) Goodfellow, R. J.; Goggin, P. L.; Duddell, D. A. *J. Chem. Soc. A* **1968**, 504.

(13) Strömberg, S.; Svensson, M.; Zetterberg, K. *Organometallics* **1997**, *16*, 3165.

(14) Sheppard, W. A. *J. Am. Chem. Soc.* **1970**, *92*, 5419. Tolman, C. A. *J. Am. Chem. Soc.* **1970**, *92*, 2953.

(15) Alonso, P. J.; Forniés, J.; García-Monforte, M. A.; Martín, A.; Menjón, B. *Organometallics* **2005**, *24*, 1269.

(16) Forniés, J.; Martín, A.; Martín, L. F.; Menjón, B.; Kalamarides, H. A.; Rhodes, L. F.; Day, C. S.; Day, V. W. *Chem. Eur. J.* **2002**, *8*, 4925. Usón, R.; Forniés, J.; Tomás, M.; Menjón, B. *Organometallics* **1986**, *5*, 1581. Usón, R.; Forniés, J.; Tomás, M.; Menjón, B. *Organometallics* **1985**, *4*, 1912.

(17) Usón, R.; Forniés, J.; Tomás, M.; Casas, J. M.; Navarro, R. *J. Chem. Soc., Dalton Trans.* **1989**, 169.

(18) Usón, R.; Forniés, J.; Tomás, M.; Casas, J. M.; Cotton, F. A.; Falvello, L. R.; Llusar, R. *Organometallics* **1988**, *7*, 2279.

(19) Usón, R.; Forniés, J.; Tomás, M.; Casas, J. M.; Cotton, F. A.; Falvello, L. R.; Feng, X. *J. Am. Chem. Soc.* **1993**, *115*, 4145.

(20) Usón, R.; Forniés, J.; Tomás, M.; Martínez, F.; Casas, J. M.; Fortuño, C. *Inorg. Chim. Acta* **1995**, *235*, 51.

shows platinum satellites with $^3J(^{195}Pt,F) = 480$ Hz, a value considerably higher than that observed for the *ortho* F atoms belonging to the mutually *trans* C_6F_5 groups, for which $^3J(^{195}Pt,F) = 311$ Hz.

The addition of ethene-saturated *n*-hexane to the reaction medium causes the precipitation of a white solid, which is identified as $[NBu_4][Pt(C_6F_5)_3(\eta^2\text{-}C_2H_4)]$ (**1**). When the mother liquor is allowed to stand at −30 °C overnight, a second fraction of **1** is additionally obtained (60% overall yield). Complex **1** stands without decomposition for several hours in solution at room temperature and can be handled in the solid state for short periods of time in the air; it is therefore reasonably stable both to heat and against the action of air.

The solid-state IR spectrum of **1** (KBr) shows a number of absorptions which are typical of the metal-coordinated C_6F_5 group. These include three strong and well-defined absorptions at 798, 785, and 775 cm^{-1}, attributable to the so-called X-sensitive vibration modes,[21] which, from a symmetry point of view, are known to behave as the M−R stretching vibrations (C_{2v}, IR active Γ_{M-R} fundamentals: $2A_1 + B_1$). No absorption in the IR spectrum of **1** could be unambiguously assigned to the ν(C=C) vibration.[22] B3LYP/LANL2DZ calculations on complex **1** predicted that the unscaled harmonic vibrational frequencies associated with the stretching vibration of the coordinated ethene ligand combined with the symmetric and asymmetric CH_2 scissoring vibrations occur at 1307 (symmetric), 1501 (asymmetric), and 1584 (symmetric) cm^{-1} as very weak absorption bands (relative intensities less than 3%). Coordination of ethene to the "$Pt(C_6F_5)_3^-$" fragment in **1** is, however, shown by ^1H and ^{13}C NMR spectroscopy. Aside from the signals corresponding to the NBu_4^+ cation, both the ^1H and $^{13}C\{^1H\}$ NMR spectra of **1** show sharp singlets at the following chemical shift values: δ_H 4.33 ppm and δ_C 78.9 ppm. Each of these signals is flanked by clearly defined platinum satellites with coupling constants $^2J(^{195}Pt,H) = 47$ Hz and $^1J(^{195}Pt,C) = 88$ Hz, respectively. All of these values are comparable with those reported for Zeise's salt: δ_H ([^{2}H]methanol) 4.36 ppm, $^2J(^{195}Pt,H) = 65.2$ Hz;[12b] $\delta_C \sim 70$ ppm, $^1J(^{195}Pt,C) \approx 195$ Hz.[23] The marked upfield shifts observed in the $[PtR_3(\eta^2\text{-}C_2H_4)]^-$ anions (R = Cl, C_6F_5) with respect to the free ethene values (δ_H 5.28 ppm, δ_C 123.3 ppm)[24] denote significant shielding effects experienced by the ligand upon coordination to the "PtR_3^-" fragments.

Synthesis and Characterization of $[NBu_4][Pd(C_6F_5)_3(\eta^2\text{-}C_2H_4)]$ (2). The analogous Pd species $[NBu_4][Pd(C_6F_5)_3(\eta^2\text{-}C_2H_4)]$ (**2**) is formed in a similar way by reaction of the corresponding dinuclear precursor $[NBu_4]_2[\{Pd(C_6F_5)_2\}_2(\mu\text{-}C_6F_5)_2]$ in CH_2Cl_2 solution with C_2H_4 at 0 °C (Scheme 2). Even at this temperature, the reaction proceeds considerably faster (5 min) than is observed for the platinum homologue at room temperature (90 min), a fact that is related to the higher reactivity usually observed for Pd as compared to that for Pt derivatives.[25] On the other hand, complex **2** is considerably less stable than **1**, since it easily reverts to the parent species under C_2H_4 release at temperatures above 0 °C or when the ethene pressure is reduced (Scheme 2).

The IR vibrational behavior of **2** is roughly similar to that observed for **1**. In this case, however, the three expected IR-active X-sensitive vibration modes of the C_6F_5 groups[21] are not well resolved, giving rise to two defined signals at 784 and 766 cm^{-1} together with a shoulder at 797 cm^{-1}. Again, an absorption corresponding to the ν(C=C) vibration could not be located with certainty in the IR spectrum of **2**. However, the predicted unscaled harmonic vibrational frequencies associated with the stretching vibration of the coordinated ethene ligand combined with the symmetric and asymmetric CH_2 scissoring vibrations in complex **2** absorb at 1337 (symmetric), 1479 (asymmetric), and 1627 cm^{-1} (symmetric) as very weak absorption bands (relative intensities less than 1%). The shifting of the ν(C=C) vibrations to higher frequencies in complex **2** relative to those of complex **1** is compatible with the C=C bond length expected in **2** being shorter than in **1** (see below).

As observed in complex **1**, the ^{19}F NMR spectrum of **2** also shows two sets of C_6F_5 signals in a 2:1 ratio. The C_2H_4 ligand gives rise to singlets in the ^1H and $^{13}C\{^1H\}$ NMR spectra of **2** at the following chemical shift values: δ_H 5.12 ppm, δ_C 97.6 ppm. The δ_H value observed for **2** is very similar to that reported for the chloro derivative $[PdCl_3(\eta^2\text{-}C_2H_4)]^-$ in [^{2}H]tetrahydrofuran solution (δ_H 5.09 ppm).[12b] The fact that the ethene ligand in the $[MR_3(\eta^2\text{-}C_2H_4)]^-$ species is considerably less shielded for Pd than for Pt can be related to the less efficient π-back-bonding ability of Pd^{II} compared with that of Pt^{II}, as will be discussed later on. Since the original formulation of the π-complex theory of metal-olefin complexes, put forward by Dewar,[7] the metal−alkene bond is considered to be the result of the following two components: (1) a dative bond from the filled π MOs of the alkene to the Lewis acidic ML_n metal fragment (σ donation), and (2) a reverse dative bond from filled orbitals of the ML_n moiety to empty π^* orbitals of the alkene (π back-donation). There is no general agreement, however, on the relative importance of these two components,[26] probably because of releasing electron density from π bonding MOs as well as adding it into π^* antibonding MOs should result in a neat C=C bond weakening. The geometry of the Pd complex

(21) Maslowsky, E., Jr. *Vibrational Spectra of Organometallic Compounds*; Wiley: New York, 1977; pp 437−442. Usón, R.; Forniés, J. *Adv. Organomet. Chem.* **1988**, *28*, 219.

(22) A weak absorption appearing at ca. 1525 cm^{-1} in the solid-state Raman spectrum of Zeise's salt has been attributed to the ν(C=C) vibration strongly coupled with CH_2 scissoring and CH_2 wagging modes: Mink, J.; Papai, I.; Gal, M.; Goggin, P. L. *Pure Appl. Chem.* **1989**, *61*, 973. However, there is no universal agreement about this kind of assignment, as discussed by: Hartley, F. R. In *Comprehensive Organometallic Chemistry*; Wilkinson, G., Stone, F. G. A., Abel, E. W., Eds.; Pergamon Press: Oxford, U.K., 1982; Vol. 6, Section 39.7.3, pp 632−680.

(23) Mann, B. E.; Taylor, B. F. *^{13}C NMR Data for Organometallic Compounds*; Academic Press: London, U.K., 1981; Table 2.10, pp 184−199.

(24) Pretsch, E.; Clerc, T.; Seibl, J.; Simon W. *Tabellen zur Strukturaufklärung organischer Verbindungen mit spektroskopischen Methoden*, 3rd ed.; Springer-Verlag: Berlin, Germany, 1986.

(25) Hartley, F. R. *The Chemistry of Platinum and Palladium*; Applied Science: London, U.K., 1973.

(26) As an example, the ethene ligand in salts of the $[PtCl_3(\eta^2\text{-}C_2H_4)]^-$ anion has been assigned a strong σ-donor and a very weak π-acceptor ability (Chang, T.-H. Zink, J. I. *J. Am. Chem. Soc.* **1984**, *106*, 287) and alternatively a good σ-donor and a strong π-acceptor character (Jaw, H.-R. C.; Chang, T.-H.; Zink, J. I. *Inorg.* Chem. **1987**, *26*, 4204). Both contradicting conclusions were drawn from the interpretation of low-temperature, single-crystal polarized electronic spectroscopy data.

Table 1. Crystal Data and Structure Refinement Details for 2

empirical formula	$C_{36}H_{40}F_{15}NPd$
fw	878.09
cryst size (mm)	0.48 × 0.31 × 0.13
temp (K)	100(1)
cryst system	triclinic
space group	$P\bar{1}$
a (pm)	979.65(7)
b (pm)	1894.69(13)
c (pm)	2108.50(14)
α (deg)	68.782(1)
β (deg)	86.598(1)
γ (deg)	89.305(1)
V (nm^3)	3.6417(4)
Z	4
d_c (g cm^{-3})	1.602
μ (mm^{-1})	0.614
F(000)	1776
θ range (deg)	2.30−25.06
index range	$-11 \le h \le 10$ $-22 \le k \le 22$ $-25 \le l \le 16$
no. of rflns collected	19 325
no. of unique rflns	12 624 ($R_{int} = 0.0263$)
completeness to $\theta = 25.03°$ (%)	98.0
no. of data/restraints/params	12 624/12/979
final R indices ($I > 2\sigma(I)$)[a]	$R1 = 0.0423$, $wR2 = 0.0982$
R indices (all data)	$R1 = 0.0589$, $wR2 = 0.1066$
GOF[b] on F^2	1.060

[a] $R1 = \sum(|F_o| - |F_c|)/\sum|F_o|$; $wR2 = [\sum w(F_o^2 - F_c^2)^2/\sum w(F_c^2)^2]^{1/2}$; $w = [\sigma^2(F_o^2) + (g_1P)^2 + g_2P]^{-1}$; $P = 1/3[\max\{F_o^2,0\} + 2F_c^2]$. [b] Goodness of fit $= [\sum w(F_o^2 - F_c^2)^2/(n_{obs} - n_{param})]^{1/2}$.

$[PdCl_3(\eta^2\text{-}C_2H_4)]^-$ has been the subject of several theoretical studies at different calculation levels.[12a,13,30,31] Since, to the best of our knowledge, only spectroscopic data are currently available for this anionic species,[12] we considered it convenient to obtain unequivocal structural information for the related $[Pd(C_6F_5)_3(\eta^2\text{-}C_2H_4)]^-$ anion.

The crystal and molecular structures of **2** have been established by X-ray diffraction methods. General crystallographic information are collected in Table 1, and a selection of bond distances and angles is given in Table 2. Two crystallographically independent $[Pd(C_6F_5)_3(\eta^2\text{-}C_2H_4)]^-$ anions were found in the asymmetric unit of the crystal but, because of their similarity, we will refer to only one of them (Figure 1). The Pd atom is in an approximately *SP*-4 environment defined by the *ipso*-C atoms of the three σ-bound C_6F_5 groups (C_6F_5-κ^1) and the midpoint between the doubly bonded C atoms of the metal π-bound ethene molecule (C_0). The C_2H_4 ligand adopts an upright coordination, the C(19)═C(20) line forming an angle of 1.8° with the normal to the Pd coordination plane. Only small angular deviations with respect to the ideal *SP*-4 geometry are observed. However, it is interesting to note that the C−Pd−C angle between the mutually *trans* C_6F_5 groups is slightly less than 180° (C(1)−Pd(1)−C(13) = 176.46(13)°), the fluoroaryl rings being bent *away* from the ethene ligand. The C_6F_5 rings are almost perpendicular to the Pd coordination plane, with which they form angles between 86.7° and 89.1°. The ethene ligand is practically eclipsed with the C_6F_5 ring in a *trans* position, the C(19)═C(20) line forming an angle of 86.2° with the normal to the referred ring. The two mutually *trans* C_6F_5 rings also adopt an almost eclipsed arrangement (interplanar angle 4.8°). The C═C bond distance (C(19)−

Table 2. Selected Interatomic Distances and Angles[a] and Their Estimated Standard Deviations for 2

Bond Distances (pm)			
Pd(1)−C(1)	206.9(4)	Pd(2)−C(21)	207.4(3)
Pd(1)−C(7)	202.8(3)	Pd(2)−C(27)	203.5(4)
Pd(1)−C(13)	206.6(4)	Pd(2)−C(33)	206.4(3)
Pd(1)−C(19)	225.4(4)	Pd(2)−C(39)	226.3(4)
Pd(1)−C(20)	225.7(4)	Pd(2)−C(40)	224.5(4)
C(1)−C(2)	138.0(5)	C(21)−C(22)	139.1(5)
C(1)−C(6)	137.8(5)	C(21)−C(26)	137.9(5)
C(2)−F(2)	137.0(4)	C(22)−F(22)	137.6(4)
C(6)−F(6)	136.7(4)	C(26)−F(26)	136.9(4)
C(7)−C(8)	138.9(5)	C(27)−C(28)	137.1(5)
C(7)−C(12)	138.1(5)	C(27)−C(32)	139.1(5)
C(8)−F(8)	135.1(4)	C(28)−F(28)	135.5(4)
C(12)−F(12)	136.4(4)	C(32)−F(32)	135.8(4)
C(13)−C(14)	137.5(5)	C(33)−C(34)	137.9(5)
C(13)−C(18)	138.7(5)	C(33)−C(38)	138.8(5)
C(14)−F(14)	136.8(4)	C(34)−F(34)	136.9(4)
C(18)−F(18)	136.8(4)	C(38)−F(38)	136.8(4)
C(19)−C(20)	133.6(6)	C(39)−C(40)	131.5(6)
C(19)−H(19A)	95.3(5)	C(39)−H(39A)	95.1(5)
C(19)−H(19B)	95.2(5)	C(39)−H(39B)	95.2(5)
C(20)−H(20A)	95.2(5)	C(40)−H(40A)	95.0(5)
C(20)−H(20B)	95.1(5)	C(40)−H(40B)	94.9(5)
Bond Angles (deg)			
C(1)−Pd(1)−C(7)	88.64(13)	C(21)−Pd(2)−C(27)	88.76(13)
C(1)−Pd(1)−C(13)	176.46(13)	C(21)−Pd(2)−C(33)	173.02(14)
C(7)−Pd(1)−C(13)	87.91(14)	C(27)−Pd(2)−C(33)	86.26(13)
C(1)−Pd(1)−C(19)	92.10(14)	C(21)−Pd(2)−C(39)	92.04(16)
C(1)−Pd(1)−C(20)	92.16(15)	C(21)−Pd(2)−C(40)	93.28(17)
C(7)−Pd(1)−C(19)	161.13(14)	C(27)−Pd(2)−C(39)	163.73(16)
C(7)−Pd(1)−C(20)	164.36(14)	C(27)−Pd(2)−C(40)	162.23(16)
C(13)−Pd(1)−C(19)	91.42(14)	C(33)−Pd(2)−C(39)	91.38(16)
C(13)−Pd(1)−C(20)	90.94(15)	C(33)−Pd(2)−C(40)	92.95(17)
C(19)−Pd(1)−C(20)	34.46(14)	C(39)−Pd(2)−C(40)	33.91(17)
Pd(1)−C(1)−C(2)	122.8(3)	Pd(2)−C(21)−C(22)	120.9(3)
Pd(1)−C(1)−C(6)	122.9(3)	Pd(2)−C(21)−C(26)	126.2(3)
C(2)−C(1)−C(6)	114.3(3)	C(22)−C(21)−C(26)	112.9(3)
Pd(1)−C(7)−C(8)	122.7(3)	Pd(2)−C(27)−C(28)	121.8(3)
Pd(1)−C(7)−C(12)	122.9(3)	Pd(2)−C(27)−C(32)	123.0(3)
C(8)−C(7)−C(12)	114.4(3)	C(28)−C(27)−C(32)	115.2(3)
Pd(1)−C(13)−C(14)	123.5(3)	Pd(2)−C(33)−C(34)	120.7(3)
Pd(1)−C(13)−C(18)	122.0(3)	Pd(2)−C(33)−C(38)	125.7(3)
C(14)−C(13)−C(18)	114.4(3)	C(34)−C(33)−C(38)	113.5(3)

[a] A correction for libration resulted in negligible differences in the geometric parameters given.

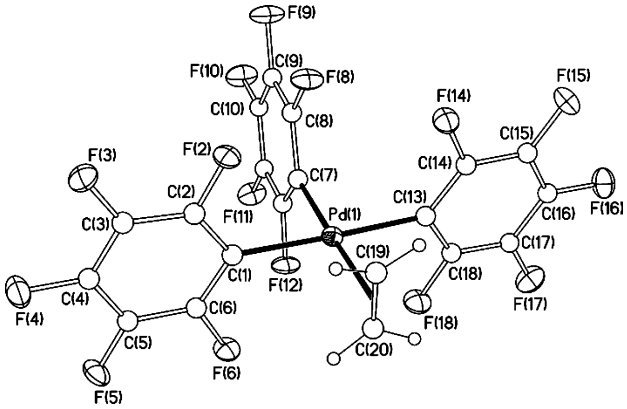

Figure 1. Thermal ellipsoid diagram (50% probability) of one of the two crystallographically independent $[Pd(C_6F_5)_3(\eta^2\text{-}C_2H_4)]^-$ anions in **2**.

(27) Bartell, L. S.; Roth, E. A.; Hollowell, C. D.; Kuchitsu, K.; Young, J. E., Jr. *J. Chem. Phys.* **1965**, *42*, 2683.
(28) The α angle is defined as in: Stalick, J. K.; Ibers, J. A. *J. Am. Chem. Soc.* **1970**, *92*, 5333.
(29) Eisenstein, O.; Hoffmann, R. *J. Am. Chem. Soc.* **1981**, *103*, 4308.
(30) Hay, P. J. *J. Am. Chem. Soc.* **1981**, *103*, 1390.
(31) Filatov, M. J.; Gritsenko, O. V.; Zhidomirov, G. M. *J. Mol. Catal.* **1989**, *54*, 462.

C(20) = 133.6(6) pm) is the same as in the free ligand (133.7(2) pm).[27] However, the C−H bonds are slightly bent away from the Pd center, the normals of the CH_2 units forming the angle α = 26.4°.[28] This α angle is twice the deviation of the CH_2 unit from the original planar arrangement. The two Pd−C(ethene) distances are identical within experimental error: Pd(1)−C(19) = 225.4(4) pm and Pd(1)−C(20) = 225.7(4) pm. These distances are considerably longer than those observed in the $[PtCl_3(\eta^2\text{-}C_2H_4)]^-$ anion, where the mean Pt−C distance is 213.1(3) pm. Longer M−C bonds and less distortion of the alkene ligand compared with that of the free molecule have been considered indicative of weaker alkene coordination. A weaker M−(η^2-C_2H_4) interaction should imply a smaller perturbation of the ethene π bonding system, as had already been predicted by extended Hückel calculations on the $[MCl_3(\eta^2\text{-}C_2H_4)]^-$ anions (M = Pd, Pt).[29] Consistent with this weak Pd−(η^2-C_2H_4) bond is the small *trans* influence exerted by the C_2H_4 ligand in **2**, showing that the C_6F_5 group acts as a better σ-donor ligand toward Pd^{II} than does the η^2-coordinated ethene molecule. Thus, the Pd−C_6F_5 bond *trans* to ethene (Pd(1)−C(7) = 202.8(3) pm) is significantly shorter than those corresponding to the mutually *trans* C_6F_5 groups (Pd(1)−C(1) = 206.9(4), Pd(1)−C(13) = 206.6(4) pm). The opposite trend was observed in Zeise's salt, where the *trans*-to-ethene Pt−Cl distance (234.0(2) pm) was found to be longer than those corresponding to the mutually *trans* Cl ligands (230.2(2) pm).[10] However, according to our B3LYP/LANL2DZ calculations on Zeise's salt under vacuum (see below), the *trans*-to-ethene Pt−Cl distance (243.1 pm) was found to be comparable to those corresponding to the mutually *trans* Cl ligands (244.5 pm). Therefore, in our opinion, the different Pt−Cl bond distances observed in Zeise's salt are most probably due to electrostatic interactions between the Cl ligands and the K^+ ions in the crystal lattice.

Spectroscopic Detection of $[NBu_4][Ni(C_6F_5)_3(\eta^2\text{-}C_2H_4)]$ (3). It is not possible to use for Ni a synthetic procedure similar to that just discussed for its heavier metal homologues because of the lack of an appropriate starting material in this case. All of our attempts to prepare the dinuclear compound $[NBu_4]_2[\{Ni(C_6F_5)_2\}_2(\mu\text{-}C_6F_5)_2]$ have failed to date. By reaction of $[NBu_4]_2[Ni(C_6F_5)_4]$[33] with *cis*-$[Ni(C_6F_5)_2(THF)_2]$[16] in noncoordinating solvents, no compound containing μ-C_6F_5 was obtained—at least under the essayed experimental conditions. A different synthetic approach was therefore needed in order to obtain the desired product $[NBu_4][Ni(C_6F_5)_3(\eta^2\text{-}C_2H_4)]$ (**3**). Given that $[NBu_4]_2[Ni(C_6F_5)_4]$ is known to react with Et_2O solutions of HCl(*g*) under a CO atmosphere, yielding $[NBu_4][Ni(C_6F_5)_3(CO)]$,[16] a similar procedure was followed using C_2H_4 instead of CO (Scheme 3); however, no evidence of **3** was found in the reaction products. Equally unsuccessful was the reaction of $[NBu_4]_2[\{Ni(C_6F_5)_2\}_2(\mu\text{-}Cl)_2]$ with AgC_6F_5 in a noncoordinating solvent under a C_2H_4 atmosphere, a procedure that is also known to render $[NBu_4][Ni(C_6F_5)_3(CO)]$ in the presence of CO (Scheme 3).[16] It becomes clear that the Ni^{II}−ethene species **3** is much more elusive than the related carbonyl derivative.

Scheme 3

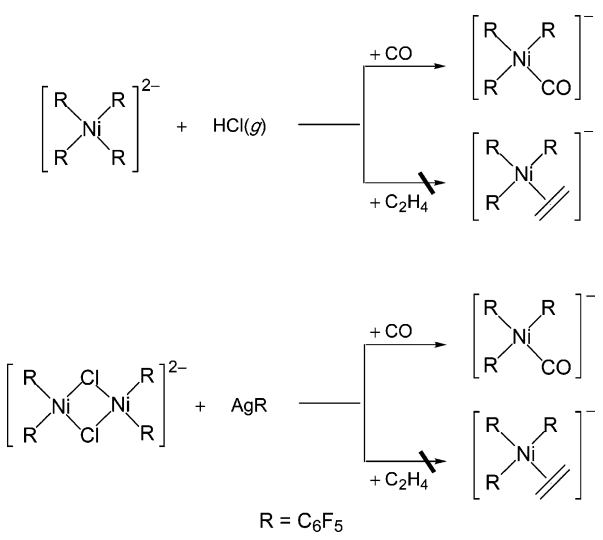

Scheme 4

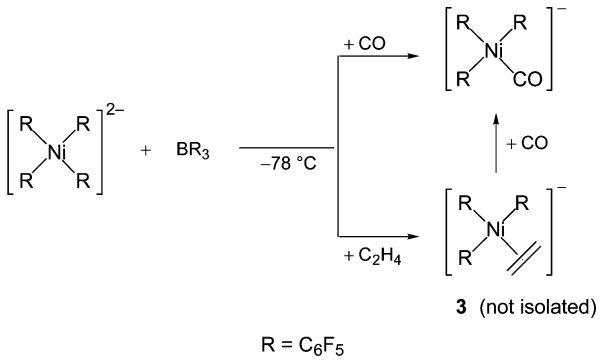

The powerful Lewis acid $B(C_6F_5)_3$ has been widely exploited as an efficient abstractor of organyl ligands in organotransition-metal chemistry.[34] To check whether it would be able to generate the "$Ni(C_6F_5)_3^-$" fragment under smooth conditions, we reacted $[NBu_4]_2[Ni(C_6F_5)_4]$ with $B(C_6F_5)_3$ in CH_2Cl_2 at −78 °C under a CO atmosphere. This reaction was found to quantitatively yield $[NBu_4][Ni(C_6F_5)_3(CO)]$ by IR and NMR spectroscopic methods (Scheme 4). If a similar reaction is carried out under a C_2H_4 atmosphere, the quantitative transformation of $[NBu_4]_2[Ni(C_6F_5)_4]$ into a single C_6F_5-containing metal species is observed by low-temperature ^{19}F NMR spectroscopy. The 2:1 integrated ratios of the two resonance signals corresponding to the *ortho* F substituents is in keeping with the formation of the desired species **3** (Scheme 4). Moreover, selective decoupling experiments demonstrate that the nuclei giving rise to those signals belong to the same spin system, since there exists detectable coupling between them (J = 22 Hz). Previous examples of through-space coupling between *ortho* F substituents of chemically nonequivalent, metal-coordinated C_6F_5 groups are already known.[35] Such a behavior was not observed in the heavier metal homo-

(32) Browning, J.; Goggin, P. L.; Goodfellow, R. J.; Norton, M. G.; Rattray, A. J. M.; Taylor, B. F.; Mink, J. *J. Chem. Soc., Dalton Trans.* **1977**, 2061.

(33) Usón, R.; Forniés, J.; Espinet, P.; Navarro, R.; Martínez, F.; Tomás, M. *J. Chem. Soc., Chem. Commun*. **1977**, 789. See also ref 16.

(34) For recent reviews, see: Erker, G. *Chem. Commun.* **2003**, 1469. Bochmann, M.; Lancaster, S. J.; Hannant, M. D.; Rodríguez, A.; Schormann, M.; Walker, D. A.; Woodman, T. J. *Pure Appl. Chem.* **2003**, *75*, 1183. Chen, E. Y.-X.; Marks, T. J. *Chem. Rev.* **2000**, *100*, 1391.

(35) Albéniz, A. C.; Espinet, P.; López-Cimas, O.; Martín-Ruiz, B. *Chem. Eur. J.* **2005**, *11*, 242.

Table 3. Selected Structural Parameters, Binding Energies ΔE, and Electronic Properties of the $[MR_3(\eta^2\text{-}C_2H_4)]^-$ (M = Ni, Pd, Pt; R = C_6F_5, Cl) Species Computed at the B3LYP/dgdzvp[a] Level of Theory

	C_6F_5/Cl		
	Ni	Pd	Pt
ΔE (kcal mol^{-1})	10.9/8.2	12.4/16.2	18.6/34.1
R_e(C−C) (pm)	136.7/137.9	136.3/137.8	139.6/142.4
R_e(M−C) (pm)	217.6/210.8	237.1/225.5	229.3/213.5
R_e(M−R_t) (pm)	193.2/222.5	208.1/237.3	205.4/243.1
R_e(M−R_c) (pm)	196.8/225.8	212.8/240.4	208.8/244.5
θ_e(C−M−C) (deg)	36.6/38.2	33.4/35.6	35.4/38.3
θ_e(R_c−M−R_c) (deg)	175.0/178.2	176.0/176.4	178.2/176.9
θ_e(R_c−M−R_t) (deg)	87.5/90.9	88.0/91.8	89.1/91.6
η (eV)	2.48/1.65	2.48/1.68	2.57/2.00
q_M[b]	0.76/0.89	0.61/0.76	0.64/0.66
q_C	−0.41/−0.44	−0.40/−0.42	−0.43/−0.48
bop(C−C)[c]	0.447/0.375	0.487/0.447	0.350/0.287
Pop(π)[d] (donor)	1.828/1.789	1.844/1.762	1.750/1.666
Pop(π^*) (acceptor)	0.129/0.192	0.103/0.123	0.194/0.337
Pop(d_{yz}) (donor)	1.853/1.830	1.882/1.833	1.788/1.695
$E(2)$[e] (kcal mol^{-1})	20.2/25.4	17.2/28.3	36.4/61.8

[a] The LANL2DZ basis set was used for the Pt compounds. [b] Natural charges. [c] Mulliken bond overlap population. [d] Electron population of the π and π^* MOs of the coordinated ethene molecule and the nonbonding d_{yz} AO (donor orbital) of the central metal atom. [e] The stabilization energy associated with the n(d_{yz}) → (π^*-MO) charge transfer (CT) interactions describing the π-back-bonding effect, which is given by $E(2) = \Delta E_{ij} = q_i(F(i,j)^2)/(\epsilon_j - \epsilon_i)$, where q_i is the donor orbital occupancy, ϵ_i and ϵ_j are diagonal elements (orbital energies), and $F(i,j)$ is the off-diagonal NBO Fock matrix element.[36]

logues **1** and **2**. [^{2}H]Dichloromethane solutions of **3** at −80 °C were found to exhibit, after removal of excess C_2H_4, a broad signal at δ_H 4.96 ppm in the ^{1}H NMR spectrum that can be assigned to the η^2-C_2H_4 ligand. Compound **3** was found to decompose in CH_2Cl_2 solution above −50 °C, giving complex mixtures of pentafluorophenyl−metal derivatives. It is interesting to note that, in such mixtures of decomposition products, the presence of high-frequency resonance signals characteristic of μ-C_6F_5 groups was observed by ^{19}F NMR spectroscopy. When CH_2Cl_2 solutions of **3** were allowed to reach room temperature under a CO atmosphere, $[NBu_4][Ni(C_6F_5)_3(CO)]$ was obtained as the only species containing metal-coordinated C_6F_5 groups (Scheme 4).

The spectroscopic, thermal, and chemical behaviors of the unstable species **3** are consistent with a formulation as $[NBu_4][Ni(C_6F_5)_3(\eta^2\text{-}C_2H_4)]$. All our attempts to isolate this compound have failed to date.

Relative Stability and Quantitative Estimates of Back-Bonding in $[MR_3(\eta^2\text{-}C_2H_4)]^-$ (M = Ni, Pd, Pt; R = C_6F_5, Cl). Our experimental results concerning the compared thermal stability of compounds **1**−**3** as well as the structural data of **2** were corroborated by DFT calculations at the B3LYP level of theory using a basis set of double-ζ valence quality analogous to that used previously in calculations on the stability of the $[MCl_3(\eta^2\text{-}C_2H_4)]^-$ anions.[13] Selected structural parameters, binding energies, and electronic properties of the $[MR_3(\eta^2\text{-}C_2H_4)]^-$ (M = Ni, Pd, Pt; R = C_6F_5, Cl) compounds are compiled in Table 3. It can be seen that the salient features of the structures of all Zeise type salts are reproduced satisfactorily by the B3LYP calculations. Interestingly, the B3LYP/dgdzvp calculations reproduce the experimentally determined C=C bond distance of 133.7(2) pm in the free ethene molecule,[27] indicating that the computational level of theory used provides reliable structural parameters for the compounds under study. For the $[Pd(C_6F_5)_3(\eta^2\text{-}C_2H_4)]^-$ compound the computed C=C bond distance of 136.3 pm is slightly longer by 2.7 pm relative to the experimental value. The same holds also true for the Pd−C(ethene) and Pd−C_6F_5 bond distances. This is not an unexpected result, since the computed structural parameters refer to an isolated molecule in the gas phase. In all of the complexes the M−R bond *trans* to the coordinated ethene molecule was predicted to be significantly shorter than those corresponding to the mutually *trans* R ligands, in line with the experimental findings. Our calculations on the $[MCl_3(\eta^2\text{-}C_2H_4)]^-$ anions are in excellent agreement with analogous calculations reported previously.[12a,13,30,31] Thus, a C=C bond length of 139.5 pm and a quite short Pd−C distance of 219.7 pm were obtained using the BP86 functional in an independent DFT calculation.[12a] In contrast, a C=C bond length of 135.4 pm, closer to our theoretical and experimental value, together with a much longer Pd−C distance of 235 pm were attained by *ab initio* calculations using a relativistic effect core potential for Pd.[30] Very similar results were attained using the CNDO-S^2 method—a semiempirical SCF MO calculation procedure.[31]

Let us now go deeper into the bonding mechanism of the coordinated ethene ligand in the novel $[M(C_6F_5)_3(\eta^2\text{-}C_2H_4)]^-$ (M = Ni, Pd, Pt) molecules and make comparisons with the $[MCl_3(\eta^2\text{-}C_2H_4)]^-$ analogues. To achieve this goal, we carried out NBO analyses of electron populations of the relevant donor−acceptor orbitals and computed the second-order stabilization energy $E(2)$ associated with the charge transfer (CT) interactions (Table 3) describing the back-bonding phenomenon.[36] It can be seen that the π-acceptor ability of the coordinated ethene molecule quantified by the electron population of the acceptor π^* MO in both series of Zeise type salts follows the trend Pt > Ni > Pd. More specifically, in the $[MCl_3(\eta^2\text{-}C_2H_4)]^-$ series, the back-bonding in the Pt compound is 2.7 and 1.8 times stronger than in the Pd and Ni compounds, respectively. On the other hand, in the $[M(C_6F_5)_3(\eta^2\text{-}C_2H_4)]^-$ series, the back-bonding effect in the Pt compound is 1.9 and 1.5 times stronger than in the Pd and Ni compounds, respectively. Noteworthy is the stronger back-bonding in $[MCl_3(\eta^2\text{-}C_2H_4)]^-$ than in the $[M(C_6F_5)_3(\eta^2\text{-}C_2H_4)]^-$ compounds, illustrating that the good π-acceptor C_6F_5 ligand exerts a weaker π back-bonding effect than does the strong π-donor Cl ligand. The difference in the extents of π back-bonding in the two series of complexes is much higher in the Pt compounds, followed by the Ni compounds, while in Pd compounds the difference is much smaller (cf. the Pop(π^*) values of 0.103 and 0.123 for R = C_6F_5, Cl, respectively). The n(d_{yz}) → (π^*-MO) charge transfer (CT) interactions describing the π-back-bonding effect stabilize the $[M(C_6F_5)_3(\eta^2\text{-}C_2H_4)]^-$ and $[MCl_3(\eta^2\text{-}C_2H_4)]^-$ complexes by 17.2−36.4 and 25.4−61.8 kcal mol^{-1}, respectively. Noteworthy is the high stabilization (61.8 kcal mol^{-1}) of the n(d_{yz}) → (π^*-MO) interactions in Zeise's salt, exhibiting the highest π back-bonding effect. In the series of the $[M(C_6F_5)_3(\eta^2\text{-}C_2H_4)]^-$ compounds the stabilization energies due to the

(36) Rauk, A. *Orbital Interaction Theory of Organic Chemistry*; Wiley: New York, 2001, p 37.

n(d_{yz}) → (π*-MO) interactions follow the trend Pt > Ni > Pd, while in the series of the $[MCl_3(\eta^2\text{-}C_2H_4)]^-$ compounds the trend is Pt > Pd > Ni.

The absolute extents of the σ-acceptor ability of the "$M(C_6F_5)_3^-$" and "MCl_3^-" fragments may be estimated by the electron population of the bonding π-MO of the coordinated ethene molecule, Pop(π) (Table 3). In the $[M(C_6F_5)_3(\eta^2\text{-}C_2H_4)]^-$ compounds the electron density transferred from the π-MO of ethene to a vacant d orbital of the metal center follows the trend Pt (0.250 |e|) > Ni (0.172 |e|) > Pd (0.156 |e|), while in the $[MCl_3(\eta^2\text{-}C_2H_4)]^-$ compounds the trend is Pt (0.334 |e|) > Pd (0.238 |e|) > Ni (0.211 |e|). In summary, the two bonding interactions in the $[M(C_6F_5)_3(\eta^2\text{-}C_2H_4)]^-$ compounds are the largest for Pt and the smallest for Pd. It should be stressed that both bonding interactions contribute to the weakening of the C=C double bond of the coordinated ethene, by removing electron density from the π-MO and adding electron density to the π*-MO. The weakening of the C=C double bond of the coordinated ethene is reflected in the computed C=C bond lengths, with the elongation of the bond (Table 3) following the trend Pt ≫ Ni > Pd in both series of compounds. Finally, the two bonding interactions are the key factors determining the stability of the Zeise type salts, both contributing to the binding energy of the ethene ligand to the metal-containing fragment. The computed binding energies (Table 3) were found in the range of 10.9−18.6 kcal mol^{-1} for the $[M(C_6F_5)_3(\eta^2\text{-}C_2H_4)]^-$ compounds and 8.2−34.1 kcal mol^{-1} for the $[MCl_3(\eta^2\text{-}C_2H_4)]^-$ species. Note the higher stability of the Pt compounds in both series of complexes. In general terms, the $[M(C_6F_5)_3(\eta^2\text{-}C_2H_4)]^-$ compounds are less stable than their corresponding $[MCl_3(\eta^2\text{-}C_2H_4)]^-$ counterparts, in line with the extents of the two bonding effects in the complexes. The Pd compounds have comparable stabilities, and therefore, both complexes should be isolable under the appropriate conditions, in line with the experimental findings. Most important is the slightly higher stability of the $[Ni(C_6F_5)_3(\eta^2\text{-}C_2H_4)]^-$ compound as compared to that of the $[NiCl_3(\eta^2\text{-}C_2H_4)]^-$ analogue. Moreover, the stability of the $[Ni(C_6F_5)_3(\eta^2\text{-}C_2H_4)]^-$ compound is comparable to that of the isolated $[Pd(C_6F_5)_3(\eta^2\text{-}C_2H_4)]^-$ anion and, therefore, the Ni complex is predicted to exist also as a stable species, thus confirming its experimental identification by NMR spectroscopy in solution reported herein.

Concluding Remarks

Suitable synthetic procedures have been devised to prepare the complete series of $[M(C_6F_5)_3(\eta^2\text{-}C_2H_4)]^-$ species for the group 10 metals (M = Ni, Pd, Pt). They are all-organometallic analogues of Zeise's salt, since the metal coordination sphere is entirely made of C-donor ligands. In contrast with the marked stability of the Pt complex **1**, the Pd derivative **2** easily evolves C_2H_4, as the result of an intermolecular substitution reaction in which the dinuclear species $[NBu_4]_2[\{Pd(C_6F_5)_2\}_2(\mu\text{-}C_6F_5)_2]$ is formed. The Ni compound **3** cannot be isolated, and it decomposes in solution at temperatures above −50 °C. The key factors determining the stability of the novel Zeise type salts **1**−**3** have been inferred using electronic structure calculation methods at the DFT level of theory. Quantitative estimates of back-bonding were also obtained using NBO analyses of electron populations of the relevant donor−acceptor orbitals and the second-order stabilization energy associated with the charge transfer (CT) interactions describing the back-bonding. Furthermore, the structural characterization of $[NBu_4][Pd(C_6F_5)_3(\eta^2\text{-}C_2H_4)]$ (**2**) by X-ray diffraction methods has enabled us to check the outcome of our theoretical calculations on the geometry of the central core of the $[Pd(C_6F_5)_3(\eta^2\text{-}C_2H_4)]^-$ anion against experiment. The C_2H_4 molecule remains essentially unaltered upon coordination to the "$Pd(C_6F_5)_3^-$" fragment: the C=C bond length is exactly the same as in the free ligand, and only a slight degree of pyramidalization is observed at the C atom with a moderate value of the α angle. It can be concluded that there is reasonable agreement between the experimentally obtained geometric parameters and those predicted by theoretical calculations.

Experimental Section

General Procedures and Materials. All reactions and manipulations were carried out under purified argon using Schlenk techniques. Solvents were dried by standard methods and distilled prior to use. The starting materials $[NBu_4]_2[\{M(C_6F_5)_2\}_2(\mu\text{-}C_6F_5)_2]$ (M = Pt, Pd),[17] $[NBu_4]_2[Ni(C_6F_5)_4]$,[16] and $B(C_6F_5)_3$[37] were prepared as described elsewhere. Elemental analyses were carried out with a Perkin-Elmer 2400-Series II microanalyzer. IR spectra of KBr disks were recorded on the following Perkin-Elmer spectrophotometers: 883 (4000−200 cm^{-1}) or Spectrum One (4000−350 cm^{-1}). NMR spectra were recorded on a Varian Unity-300 or on a Bruker ARX 300 spectrometer. Unless otherwise stated, the spectroscopic measurements were carried out at room temperature.

Synthesis of $[NBu_4][Pt(C_6F_5)_3(\eta^2\text{-}C_2H_4)]$ (1). A CH_2Cl_2 solution (7 cm^3) of $[NBu_4]_2[\{Pt(C_6F_5)_2\}_2(\mu\text{-}C_6F_5)_2]$ (87.6 mg, 0.047 μmol) was stirred at room temperature under an ethene atmosphere for 90 min, during which time the initially bright yellow solution gradually turned colorless. The addition of C_2H_4-saturated *n*-hexane (30 cm^3) to the resulting mixture caused the precipitation of a small amount of white solid. After this suspension was allowed to stand at −30 °C overnight, the white solid was filtered and dried at room temperature (**1**·CH_2Cl_2: 54 mg, 5 μmol, 60% yield). Anal. Found: C, 42.2; H, 3.95; N, 1.4. Calcd for $C_{37}H_{42}ClF_{15}NPt$: C, 42.25; H, 4.0; N, 1.3. IR (KBr): $\tilde{\nu}_{max}/cm^{-1}$ 1504 (vs), 1455 (vs), 1057 (vs), 956 (vs; C_6F_5: C−F),[21] 881 (m; NBu_4^+), 798 (s; C_6F_5: X-sensitive vibr),[21] 785 (s; C_6F_5: X-sensitive vibr), 775 (s; C_6F_5: X-sensitive vibr). ^1H NMR ([^2H]chloroform):[38] δ 4.33 (s, $^2J(^{195}Pt,H)$ = 47 Hz). $^{13}C\{^1H\}$ NMR ([^2H]dichloromethane):[38] δ 78.9 ($^1J(^{195}Pt,C)$ = 88 Hz). ^{19}F NMR ([^2H]chloroform): δ −117.80 ($^3J(^{195}Pt,F)$ = 480 Hz, 2F, *o*-F), −120.39 ($^3J(^{195}Pt,F)$ = 311 Hz, 4F, *o*-F), −164.42 (2F, *p*-F), −165.00 (1F, *p*-F), −165.41 (4F, *m*-F), −166.18 (2F, *m*-F).

Synthesis of $[NBu_4][Pd(C_6F_5)_3(\eta^2\text{-}C_2H_4)]$ (2). A CH_2Cl_2 solution (5 cm^3) of $[NBu_4]_2[\{Pd(C_6F_5)_2\}_2(\mu\text{-}C_6F_5)_2]$ (0.23 g, 0.13 mmol) was stirred at 0 °C under an ethene atmosphere for 5 min. Then, C_2H_4-saturated *n*-hexane (30 cm^3) was added to the reaction medium. After the resulting mixture was allowed to stand at −30 °C for 3 days, a white solid formed that was filtered and dried at −30 °C (**2**: 0.13 g, 0.15 mmol, 55% yield). Anal. Found: C, 49.2; H, 4.6; N, 1.6. Calcd for $C_{36}H_{40}F_{15}NPd$: C, 49.2; H, 4.6; N, 1.6. IR (KBr): $\tilde{\nu}_{max}/cm^{-1}$ 1497 (vs), 1456 (vs), 1056 (s), 1041 (s), 953 (vs; C_6F_5: C−F),[21] 881 (m; NBu_4^+), 797 (sh; C_6F_5: X-sensitive vibr),[21] 784 (s; C_6F_5: X-sensitive vibr), 766 (s; C_6F_5: X-sensitive vibr).[21] ^1H NMR ([^2H]dichlo-

(37) Massey, A. G.; Park, A. J. *J. Organomet. Chem.* **1964**, *2*, 245.
(38) Resonances due to the cation NBu_4^+ have been omitted.

romethane, −40 °C):[38] δ 5.12. $^{13}C\{^1H\}$ NMR ([^{2}H]dichloromethane, −40 °C):[38] δ 97.6. ^{19}F NMR ([^{2}H]dichloromethane, −40 °C): δ −114.12 (2F, *o*-F), −116.36 (4F, *o*-F), −163.26 (2F, *p*-F), −164.14 (5F: 4*m*-F + 1*p*-F), −165.05 (2F, *m*-F).

Single crystals suitable for X-ray diffraction purposes were obtained by slow diffusion of a C_2H_4-saturated *n*-hexane layer (10 cm^3) into a solution of 20 mg of **2** in CH_2Cl_2 (2 cm^3) at −30 °C.

Crystal Data for 2. Crystal data and other details of the structure analysis are presented in Table 1. All diffraction measurements were made at 100 K on a Bruker Smart CCD area detector diffractometer using graphite-monochromated Mo Kα radiation. The diffraction frames were integrated using the SAINT package[39] and corrected for absorption with SADABS.[40] Lorentz and polarization corrections were applied. The structure was solved by Patterson and Fourier methods and refined using the SHELXL-97 program.[41] All non-hydrogen atoms were assigned anisotropic displacement parameters. The hydrogen atoms were constrained to idealized geometries and assigned isotropic displacement parameters equal to 1.2 times the U_{iso} values of their respective parent atoms (1.5 times for C*H*$_3$). The positions of the hydrogen atoms of the ethene ligands were found in the electron density maps and subsequently refined with the C−H distances and H−C−H angles restrained to sensible values. Full-matrix least-squares refinement on F^2 of this model converged to final residual indices given in Table 1. CCDC reference number: 266540.

Synthesis of [NBu$_4$][Ni(C$_6$F$_5$)$_3$(η^2-C$_2$H$_4$)] (3). A CH_2Cl_2 solution (10 cm^3) of $[NBu_4]_2[Ni(C_6F_5)_4]$ (0.38 g, 0.32 mmol) was cooled at −78 °C and put under an ethene atmosphere. Then a precooled (−78 °C) solution of $B(C_6F_5)_3$ (0.18 g, 0.35 mmol) in CH_2Cl_2 (10 cm^3) was added. After 1 h of reaction, **3** was the only species detected in solution that contains metal-coordinated C_6F_5 groups. ^1H NMR ([^{2}H]dichloromethane, −80 °C):[38] δ 4.96. ^{19}F NMR ([^{2}H]dichloromethane, −80 °C):[42] δ −116.64 (pseudo quartet, 2F, *o*-F), −119.05 (pseudo triplet, 4F, *o*-F).

Computational Methods. DFT calculations at the B3LYP level of theory were carried out on the $[MR_3(\eta^2\text{-}C_2H_4)]^-$ anionic species (M = Ni, Pd, Pt; R = Cl, C_6F_5) using the GAUSSIAN03 program suite.[43] The geometries of all species were fully optimized by Becke's three-parameter hybrid functional[44,45] combined with the Lee−Yang−Parr[46] correlation functional, using a basis set of double-ζ quality (DZVP basis set)[47] for the Ni and Pd compounds, while the LANL2DZ basis set, being also of double-ζ quality, was used for the Pt compounds. Full geometry optimization was performed for each structure using Schlegel's analytical gradient method,[48] and the attainment of the energy minimum was verified by calculating the vibrational frequencies that result in the absence of imaginary eigenvalues. The computed electronic energies were corrected for zero-point energy (ZPE) differences. The stabilization energy $E(2)$ associated with the charge transfer (CT) interactions between the relevant donor−acceptor orbitals was computed from the second-order perturbative estimates of the Fock matrix in the natural bond orbital (NBO) analysis.[48,50]

Acknowledgment. This work has been supported by the Spanish MCYT (DGI)/FEDER (Project BQU2002-03997-CO2-02) and Promerus LLC.

Supporting Information Available: Crystallographic data (CIF) for [NBu$_4$][Pd(C$_6$F$_5$)$_3$(η^2-C$_2$H$_4$)] (**2**) and Cartesian coordinates and energies of the Zeise type salts (Tables S1 and S2, respectively). This material is available free of charge via the Internet at http://pubs.acs.org.

OM0502077

(39) SAINT, version 6.02; Bruker Analytical X-ray Systems, Madison, WI, 1999.

(40) Sheldrick, G. M. SADABS empirical absorption program, version 2.03; University of Göttingen, Göttingen, Germany, 1996.

(41) Sheldrick, G. M. SHELXL-97, Program for the refinement of crystal structures from diffraction data; University of Göttingen, Göttingen, Germany, 1997.

(42) No clear-cut distinction could be made between the signals corresponding to C_6F_5 groups attached to boron or nickel in the high-field region, due to extensive superposition. This circumstance precluded the reliable assignment of the *meta* F and *para* F signals for compound **3**.

(43) Frisch, M. J. T.; et al. *Gaussian 03*, Revision B.02; Gaussian, Inc.: Pittsburgh, PA, 2003. See the Supporting Information for the remaining 80 authors.

(44) Becke, A. D. *J. Chem. Phys.* **1992**, *96*, 215.

(45) Becke, A. D. *J. Chem. Phys.* **1993**, *98*, 5648.

(46) Lee, C.; Yang, W.; Parr, R. G. *Phys. Rev. Lett.* **1998**, *B37*, 785.

(47) (a) Godbout, N.; Salahub, D. R.; Andzelm, J.; Wimmer, E. *Can. J. Chem.* **1992**, *70*, 560. (b) Sosa, C.; Andzelm, J.; N.; Elkin, B. C.; Wimmer, E.; Dobbs, K. D.; Dixon, D. A. *J. Phys. Chem.* **1992**, *96*, 6630.

(48) Schlegel, H. B. *J. Comput. Chem.* **1982**, *3*, 214.

(49) Weinhold, F. In *The Encyclopedia of Computational Chemistry*; Schleyer, P. v. R., Ed.; Wiley: Chichester, U.K., 1998; pp 1792−1811.

(50) Reed, A. E.; Curtiss, L. A.; Weinhold, F. *Chem. Rev.* **1988**, *88*, 899.